RSC Advances

ROYAL SOCIETY OF CHEMISTRY

www.rsc.org/advances

Facile synthesis of nickel hydroxide-graphene nanocomposites for insulin detection with enhanced electrooxidation properties

Yuqing Lin [a,*], Lianglu Hu[b], Linbo Li[a], Keqing Wang[a]

[a]*Department of Chemistry, Capital Normal University, Beijing 100048, China*

[b]*College of Chemistry and Materials Science, Anhui Normal University, Wuhu 241000,China*

Corresponding author

Tel.: +86 1068903047; Fax:+86 1068903047

E-mail address: linyuqing@cnu.edu.cn(Y. Lin).

This study describes a facile and effective one-pot route to synthesize structurally uniform and electrochemically active nickel hydroxide-graphene nanocomposites ($Ni(OH)_2$-GN) and investigates the electrocatalytic activity toward the oxidation of insulin. Graphene here was used to tether Ni^{2+} precursor onto surfaces and eventually on-spot grow $Ni(OH)_2$ nanoparticles to form hybrid materials. The synthetic $Ni(OH)_2$-GN nanocomposite has a uniform surface distribution, which was characterized with scanning electron microscopy (SEM). Moreover, the composition of synthetic $Ni(OH)_2$-GN nanocomposite were characterized by X-ray photoelectron spectroscopy (XPS) and Fourier transform infrared spectroscopy (FT-IR spectra). The $Ni(OH)_2$-GN were electrochemically treated in 0.1 M NaOH solution through cyclic voltammograms, and then gradually transited into nickel oxyhydroxide-graphene nanocomposites (NiOOH-GN), which demonstrated high catalytic activity and improved stability to insulin oxidation. The steady-state current response increases linearly with insulin concentration from 800 nM to 6400 nM with a fast response time of less than 2s and the detection limit to be 200 nM. The excellent performance of insulin sensor including long term stability can be ascribed to the synergy effects of the large surface area (resulting in high loading ability), dispersing ability and conductivity of graphene and the large surface-to-volume ratio and electrocatalytic activity of $Ni(OH)_2$ nanoparticles.

Introduction

Insulin is an important polypeptide hormone that is used to regulate blood glucose by signaling when high levels of blood glucose are present in the body. [1-5] It is reported that the prevalence of diabetes for all age groups worldwide is estimated at 2.8% for 2000 rising to 4.4% in 2030. [6] In addition, insulin serves as a predictor of diabetes of insulinoma and trauma. [7-8] As a result, the detection of insulin is of great importance for clinical diagnostics, medical and physiological studies on diseases. The methods for detection of insulin mainly include bioassays, immunoassays and chromatography.[4] While these current technologies on the detection of insulin are slow, somewhat complex, time-consuming and special instruments as well as derivatization materials needed.

Zhang etc. studied of insulin electrooxidation at electrode and found there was an implied the electrode process with an H^+/e^- ratio equal to 1, which could be induced the oxidation process involves redox-active tyrosine residues in the insulin molecule. [2] The oxidation of the amino acid tyrosine involves its hydroxyl group and results in a release of a proton; i.e., C-OH ---->C=O + H^+ + e^-. Direct detection of insulin by electrochemical means such as on glassy carbon surface offers an excellent opportunity for the development of fast, sensitive and inherent simple systems. This approach however falls in its drawbacks such as slow oxidation kinetics and surface fouling, which are overcome by complex surface modification [9-11] and/or the use of mediators. Recently, all sorts of materials such as silica gel, [9] cobalt oxide nanoparticles [11] and carbon nanotube [2,10] etc. were also used as an electrode modifier for oxidation of insulin. Although the modified electrodes have been successfully employed for monitoring insulin, they usually fall into several disadvantages, such as reduced stability of mediators and electrocatalysts, and progressive fouling of electrode surface during insulin oxidation, or both, resulting in low sensitivity and poor reproducibility.[12-14] As a result, electrochemical catalysts to accelerate electrontransfer have been urgently hunted and used for electrooxidation and determination of insulin.

Graphene is a single layer of carbon atoms tightly packed into a two-dimensional honeycomb lattice structure of a novel carbon material. [15-17] Recently, graphene has drawn tremendous attention in many fields such as nanomaterials, nanotechnology, sensors, etc. [18-20] due to its ultra-high specific surface area and can act as an ideal base for nanocomposites. Moreover, high electron conductivity, fast heterogeneous electron-transfer rate endow graphene a robust atomic-scale scaffold for nanoparticles to form hybrid materials with improved properties. [21, 22] So far, graphene has been developed as a burgeoning support to disperse and stabilize metal, metal oxide, and semiconductor nanomaterials, such as Ag, Au, Pt, $Ni(OH)_2$. [23, 24]

Inorganic nanomaterials, such as Cu, Fe, Ni, and their oxides and sulfides, have attracted considerable attention as sensors and biosensors due to their low cost, high specific surface area, good electrocatalytic activity, and thepossibility of promoting electron transfer rates. [25-27] Recently, some forms of Ni and $Ni(OH)_2$ nanomaterials have been utilized in fabrication of biosensors due to its inexpensive, nontoxic and readily stored properties. [28-30] Unfortunately, van der Waals force between nanoparticles causes strong aggregation, which prevents effective catalytic contribution of each nanocatalyst. [31, 32] In addition, due to the semiconductivity of $Ni(OH)_2$, they are not favorable for applications in electrode materials for electrocatalysis. Thus, it is highly desirable to construct well-dispersed nanocatalysts on electronically conductive support to reduce ohmic resistance and improve the electrochemical activity. Dai's group reported a two-step method to grow $Ni(OH)_2$

nanocrystals on graphene by hydrolysis of $Ni(CH_3COO)_2$ at 80 °C in a mixed *N*,*N*-dimethylformamide/H_2O solvent and followed by dispersing the products in pure H_2O for hydrothermal treatment at 180 °C, during which the small $Ni(OH)_2$ particle coated on graphene.[33] Duan's group demonstrated a one-step hydrothermal strategy to prepare 3D graphene/$Ni(OH)_2$ composite hydrogels by heating a homogeneous aqueous mixture of graphene oxide, $Ni(NO_3)_2$, ammonia and hydrazine at 180 ℃ for 2 h.[34] Li's group synthesized a reduced graphene oxide-$Ni(OH)_2$ nanocomposite by in which Ni^{2+} was first adsorbed onto monodispersed single layer graphene oxide (GO) sheets with PVP as the surfactant and then react with hydrazine and an ammonia solution at 95 °C, $Ni(OH)_2$ nanoplates were formed and assembled onto the reduced GO nanosheets that had been reduced by hydrazine from GO.[35] However, these synthesis process still need improvement considering more simple and involving less processes and reagents. Moreover, most graphene/$Ni(OH)_2$ composite are used as supercapacitor electrode materials for energy storage while acting as electrocatalyst for protein oxidation is rarely reported.

This study describes a facile one-pot method to synthesize $Ni(OH)_2$-GN nanocomposite sensitive to insulin electrooxidation. In the $Ni(OH)_2$-GN composite material, nanoparticles of $Ni(OH)_2$ are uniformly and directly grown on highly conducting graphene. The graphene sheets overlap with each other to afford a three-dimensional conducting network for fast electron transfer between the active materials and the insulin. The as-prepared $Ni(OH)_2$-GN nanocomposites combine the dispersion characteristic, high conductivity as well as large surface area of graphene

and the catalytic property of NiOOH, and exhibit excellent catalytic performance to construct an insulin sensor. This sensor showed high stability and fast amperometric response toward insulin detection. In contrast, pure graphene, pure $Ni(OH)_2$ nanoaggregates and $Ni(OH)_2$ nanoaggregates physically mixed with graphene sheets all showed inferior performance to insulin electrochemical oxidation compared to $Ni(OH)_2$ nanoparticles directly synthesized on highly conducting graphene sheets.

Experimental

Apparatus and electrodes

Electrochemical measurements were performed with a computer-controlled electrochemical analyser (CHI 600E, Chenhua, China) and a computer-controlled advanced electrochemical system (Princeton Applied Research (PARSTAT 2273)) in a two-compartment electrochemical cell with a bare or modified GCE (3 mm in diameter) working electrode, a platinum wire counter electrode, and an (Ag/AgCl)/V (KCl-saturated) reference electrode. All of the electrochemistry experiments were performed at room temperature.

Reagents

$NiCl_2$ $6H_2O$ and porcine insulin (5733, >27 USP units mg^{-1}) were from Aladdin. Graphene were obtained from Beijing Daoking Co. Note: graphene used in this study is from chemical reduction of graphene oxide and it may still lightly oxidized. All other chemicals (analytical grade) were purchased from Beijing Chemical Reagent Company (Beijing, China) and used without further purification. Ultra-pure water was

obtained with a Milli-Q plus water purification system (Millipore Co. Ltd., USA, 18 MW).

Sample characterization

SEM (Scanning Electron Microscopy) images were obtained using Hitachi S-2600N scanning electron microcopy. FT-IR (Fourier Transform Infrared Spectroscopy) spectra were collected using a Bruker Vector 22 FTIR spectrometer in the frequency range of 4000-500 cm-1. XPS (X-ray Photoelectron Spectroscopy) measurements were carried out on a VG Microtech ESCA 2000 using a monochromic Al X-ray source.

Synthesis of $Ni(OH)_2$-GN

20 mg of graphene powders was dispersed in 10 ml deionized water by ultra-sonication for 1 h while 32.5 mg of $NiCl_2\ 6H_2O$ was dissolved in 5 ml of deionized water. After mixing these two solutions under 30 min of vigorous agitation, 0.1 M NaOH solution was introduced dropwise into the mixture to adjust pH to 11. Then the solution was heated at 50 °C for 30 min under magnetic stirring, followed by refluxing for 8 h. At last, green precipitate was obtained and rinsed with ethanol and deionized water several times. The resulting nanocomposites were dried under vacuum at 60 °C for 24 h. For the synthesis process of pure $Ni(OH)_2$, the conditions are same except for without graphene in the system.

Preparation of the insulin sensor

In an electrochemical experiment, a GC (glassy carbon) electrode was polished with 1.0, 0.3 and 0.05 μm alumina slurry to a mirror-like, respectively, followed by

rinsing thoroughly with deionized water. Then 10 μL of the $Ni(OH)_2$-GN suspension 5 mg/μL in DMF was dropped onto the GCE surface, which was exposed to air to evaporate the solvent. Then the electrode was rinsed thoroughly with deionized water to remove the physically adsorbed materials to form the $Ni(OH)_2$-GN /GC electrode for insulin sensing.

Results and Discussion

Morphology and composition of the $Ni(OH)_2$-GN

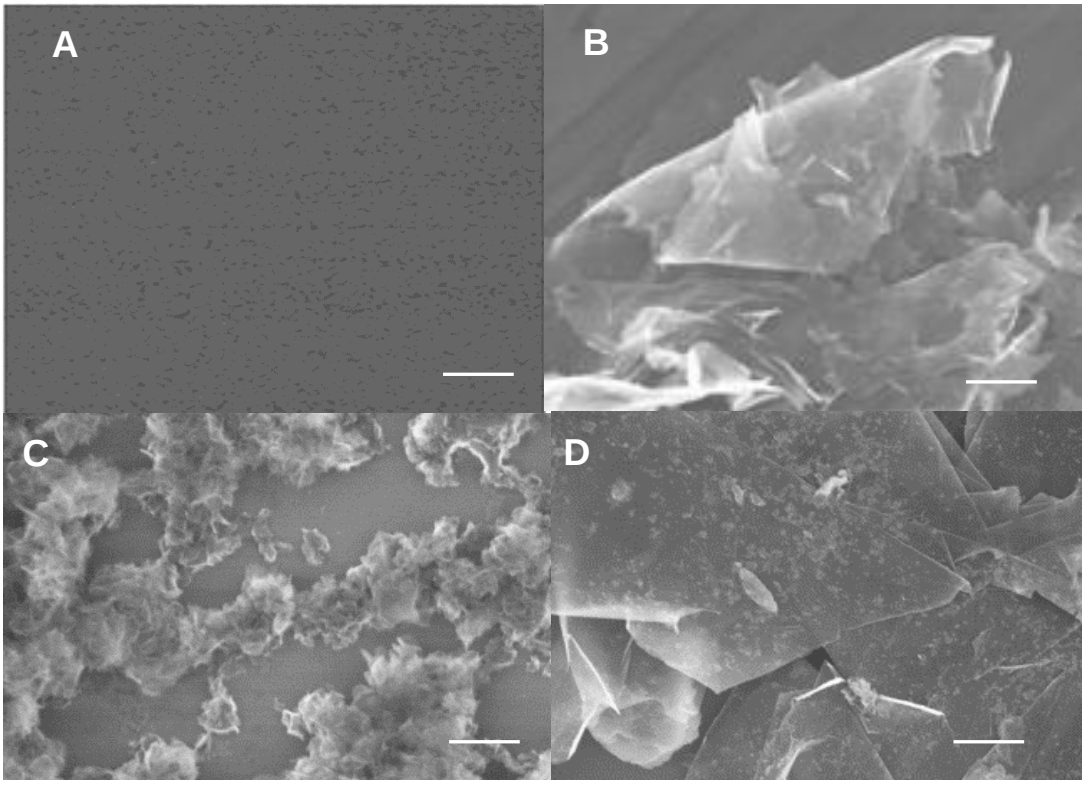

Fig. 1. FE-SEM images of (A) ITO substrate, (B) graphene-sheet, (C) as-formed $Ni(OH)_2$ and (D) $Ni(OH)_2$-GN.All scale bars represent 400 nm.

Fig.1 shows the SEM images of the blank ITO substrate (A), graphene sheet (B),

as-formed $Ni(OH)_2$ (C) and $Ni(OH)_2$-GN (D). The ITO substrate in Fig. 1A is smooth and apparently has no nano-structured material. When graphene film is coated on the surface of ITO substrate in Fig. 1B, some sheets structures are found as the texture of single-atom thick substrate, denoting the presence of graphene sheet. Fig. 1C refers to the prepared $Ni(OH)_2$ nanoparticals without the presence of graphene, apparently, $Ni(OH)_2$nanoparticals are in large size, in average diameter 50 nm and much more prone to aggregated compared with Fig 1D. While, in the $Ni(OH)_2$-GN (Fig.1D), single-crystalline nanoparticle of $Ni(OH)_2$ with diameter to be 5 nm are uniformly decorated on highly conducting graphene, demonstrating nickel ion convert to nickel hydroxide in the graphene surface. The graphene sheets overlap with each other to afford a three-dimensional conducting network for fast electron transfer between the active materials, $Ni(OH)_2$, which may improves the efficiency of electro-catalytic.

In order to prove the presence the $Ni(OH)_2$ in the graphene nanocomposites, the XPS spectra were investigated in Fig. 2A. XPS was used to obtain semiquantitative data on the chemical compositions of obtained samples. Fig.2A. Compare the representative XPS survey spectra of $Ni(OH)_2$-GN and GN, the existence of C and O are clearly observed for both samples while the Ni peaks are only obviously appearing in $Ni(OH)_2$-GN, confirming the successful incorporation of the Ni element into the nanocomposite in this study. Moreover, XPS spectra show that the characteristic of Ni 2p appears Ni 2p3/2 at 856.75eV, which is consistent with the presence of $Ni(OH)_2$. [36] The content of carbon was calculated to be 91.4%, and the content of oxygen was calculated to be 7.8% in graphene-$Ni(OH)_2$ nanocomposite while, the content of

carbon was calculated to be 91.7% and the content of oxygen was calculated to be 8.3% in graphene. The relative content of carbon and oxygen decrease after graphene are incorporated with $Ni(OH)_2$ particles demonstrate that Ni element is successfully in situ grown on graphene surface. The IR spectrums obtained for $Ni(OH)_2$-GN and graphene sample are shown in Fig. 2B. There are obvious peaks at 3643cm^{-1}, 3442cm^{-1}, 1631cm^{-1}, 1442cm^{-1}, 1117cm^{-1},which are separately assigned to the stretching and bending vibrations of free O-H and the certain O-H of H-bonded, C=C stretching carbonyl-conjugated, -CH_2 and the C-O stretching. The spectrum of the $Ni(OH)_2$-GN sample obtained is similar to that graphene except that the new peak corresponding to O-H stretching observed at 3643 cm^{-1}, which is associated with the OH vibrations confirming the presence of $Ni(OH)_2$in the composite. [37] This suggests that $Ni(OH)_2$ nanoparticles are successfully decorated onto the graphene sheets and without changing the chemistry environment of graphene.

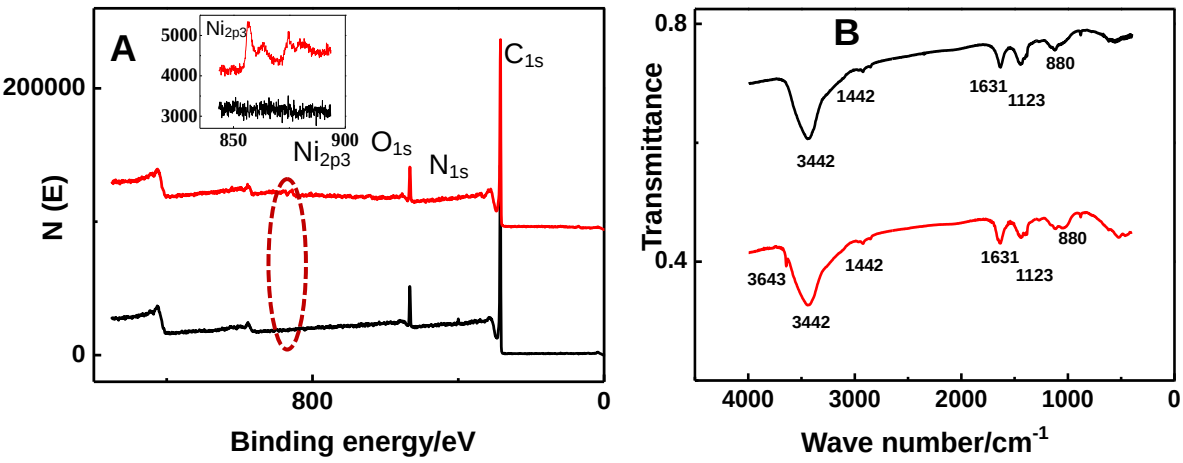

Fig 2. (A) Representative XPS survey spectra of graphene-$Ni(OH)_2$

nanocomposite (red line) and graphene (black line), inset is the zoom of XPS scans over Ni_{2p3} peak in the dotted-line marked region.(B) FT-IR spectra of graphene-$Ni(OH)_2$(red line) and graphene sheet(black line).

Electrochemical characterization of the $Ni(OH)_2$-GN /GC electrode

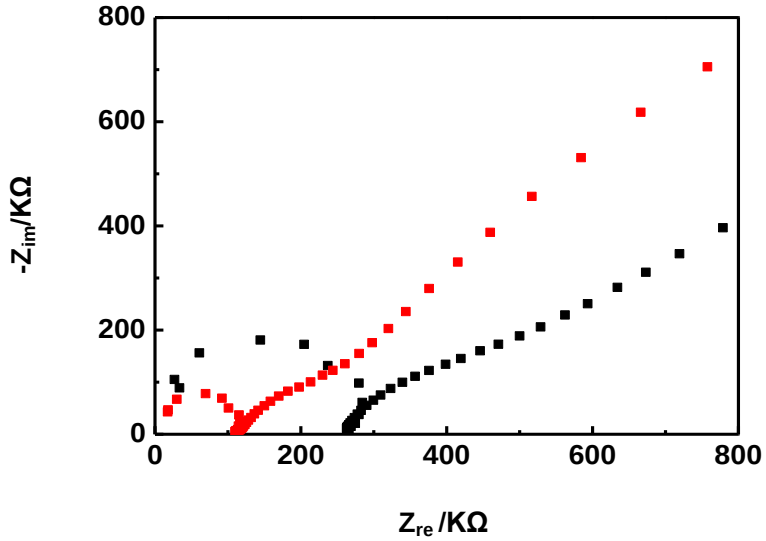

Fig 3. EIS obtained at the different electrodes: bare GC (black line) and $Ni(OH)_2$-GN (red line).

The electron transfer properties of the electrode after different surface modifications were characterized by electrochemical impedance spectroscopy (EIS) (Fig. 3). In general, the linear portion of the EIS represents the diffusion-limited process, and the semicircle portion corresponds to the electron transfer-limited process. The charge transfer resistance (Rct) at the electrode surface is equal to the semicircle diameter. A small well-defined semicircle with Rct of 268 Ω at higher frequencies was obtained for the bare GCE, which indicated a small interface electron transfer resistance. When $Ni(OH)_2$-GN was immobilized on the GC electrode surface, the high frequency part in EIS was nearly a straight line, and the Rct value decreased

to 108 Ω, which suggested that $Ni(OH)_2$-GN can improve the conductivity and electron transfer process. These results also demonstrated that $Ni(OH)_2$-GN was successfully immobilized on the GCE surface.

Electrochemical treatment on $Ni(OH)_2$-GN to form NiOOH-GN

The NiOOH-GN layer was generated using cyclic voltammetry on $Ni(OH)_2$-GN modified electrode at potential range+0.25 to +0.6 V in pH 13 solution, as shown in Fig. 4. The oxidation and reduction process of $Ni(OH)_2$ was studied in three different peaks in cyclic voltammetrys. Basically, the electrocatalytic oxidation mechanism of the $Ni(OH)_2$nanocrystal modified electrode can be explained by the following equations. [38]

$Ni(OH)_2 \rightleftharpoons NiOOH + e^-$

Firstly, at potential 0.42V, $Ni(OH)_2$-GN was oxidized at the electrode surface to NiOOH-GN. Then NiOOH-GN was reduced back to $Ni(OH)_2$-GN at 0.37V, which would be electrochemically reoxidized in the anodic scan. With the increase of the cycle number, the Ni(II) has been transferred to Ni(III), and Ni(III) is revert to Ni(II) at less positive potential. Meanwhile, the peak observed at 0.27V during the cathodic process originates from the reduction of molecular oxygen, which was produced and adsorbed on the electrode surface during the anodic scan. As a characteristic of conducting film formation, the cathodic and anodic waves grew with the number of scans up to the 300th cycle and then a current plateau and stable voltammetric response was obtained.

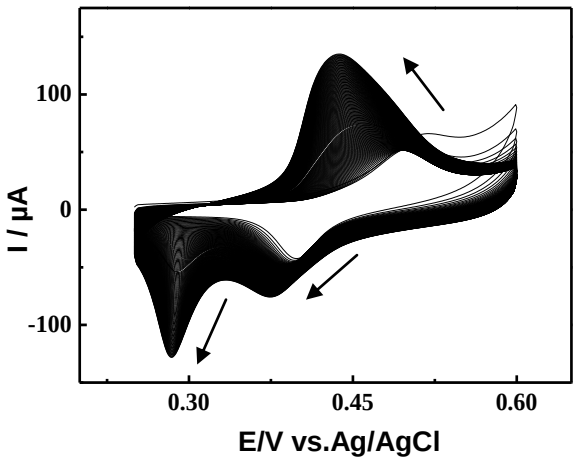

Fig 4. Cyclic voltammograms of Graphene-NiOOH film growth on a carbon composite electrode in 0.1 M NaOH solution. The potential was continuously cycled at a scan rate of 100 mV s^{-1}between 0.25V and 0.7 V vs Ag/AgCl reference electrode.

Electrocatalyticoxidation of insulin at the NiOOH-GN modified GCE

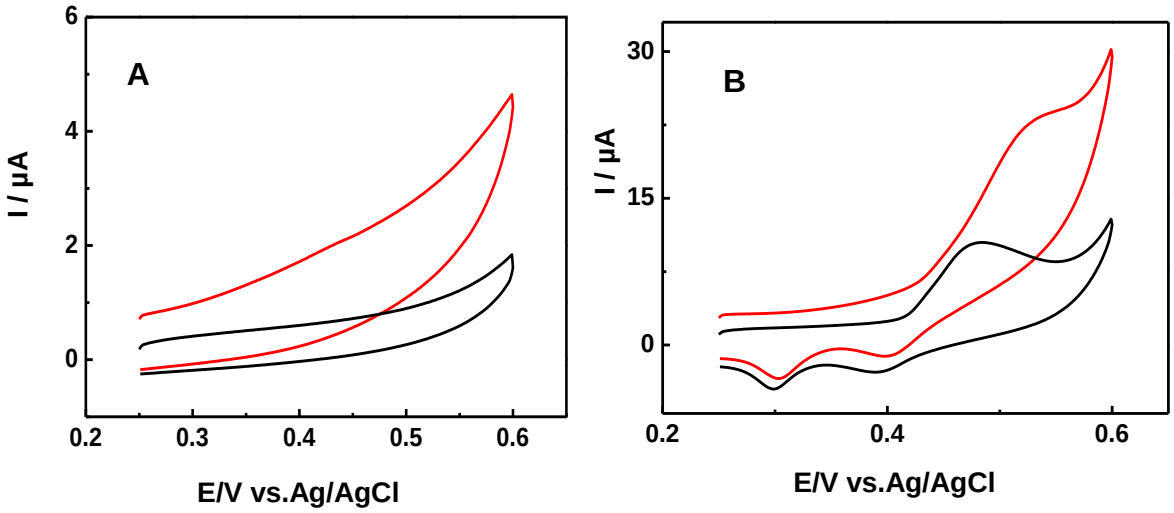

Fig 5. (A) Voltammetric response of graphene modified GCE placed in just 0.1M NaOH solution and 80 µM insulin 0.1 M NaOH solution, scan rate of 100 mV s^{-1}.(B)Voltammetric response of graphene-NiOOH modified GCE placed in just 0.1 M NaOH solution and 80 µM insulin 0.1M NaOH solution, scan rate of 100 mV s^{-1}.

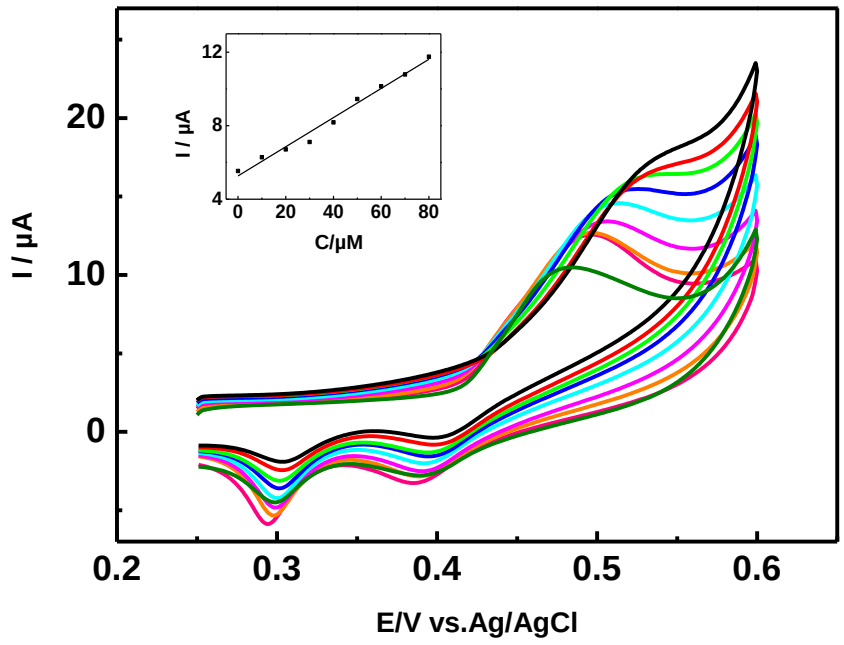

Fig 6. Voltammetric response of graphene-NiOOH modified GCE placed in 80 μM insulin 0.1 M NaOH solution at a scan rate of 50 mV s^{-1} to additions of insulin, from inner to outer 0, 10, 20, 30, 40, 50, 60, 70 and 80 μM. Inset: plot of insulin peak current versus insulin concentration.

In order to investigate the electrocatalytic activity of the formed NiOOH-GN modified electrodes, cyclic voltammograms were obtained in the presence and absence at graphene and NiOOH-GN modified electrodes. Fig.5A shows the recorded cyclic voltammograms of electrode modified with only graphene in the absence and presence of insulin in 0.1 M NaOH solution. There is no obvious anodic or reduction peak in the presence of 80μM insulin at the potential range from 0.25 to 0.60 V. While in Fig.5B, it shows the recorded cyclic voltammograms of electrode modified with NiOOH-GN, there isa dramatic enhancement in anodic peak current in the addition of 80μM insulin, indicating a strong catalytic effect of NiOOH-GN to insulin oxidation. The enhancement peak current for insulin oxidation is achieved with the modified

electrodes. The effect of adding insulin to the system was investigated in the range 0-80 μM (Fig.6). A linear dependence of the catalytic oxidation currents versus concentration of insulin can be fitted in the equation (Ip(μA)=5.27+0.079$C_{insulin}$(μM), R=0.993). Ultra-high specific surface area, high electron conductivity and fast heterogeneous electron-transfer rate endow graphene a robust atomic-scale scaffold for nanoparticles to form hybrid materials with improved properties. In addition, NiOOH nanoparticals with high catalytic activity to insulin oxidation make the NiOOH-GN composites exhibit superior catalytic activity to insulin oxidation.

Amperometric detection of insulin at NiOOH-GN modified GCE

Fig. 7 shows the amperometric response of NiOOH-GN on successive addition of insulin into 0.1 M NaOH solution (pH 13) at an applied potential of 0.51V. When insulin was added to the stirring NaOH solution, $Ni(OH)_2$-GN responded rapidly and achieved the maximum steady-state current in less 3 s. Catalytic currents showed linear response from 800nM to 6400nM (Ip(μA) = 0.08 +0.05C insulin(μM), R= 0.98) with detection limit to be 200 nM. On the other hand, the NiOOH-GN nanocomposite imparts higher stability onto amperometric measurements of insulin. Fig.7B displays the stability of the response to 7μM insulin during long-time experiment. The response remains relatively stable throughout the entire 1 hour. Moreover, pure nickel hydroxide particles were synthesized using the same method as the $Ni(OH)_2$-GNnanocomposite. When the synthetic nickel hydroxide particles were modified onto GC electrode, they were easier to drop off from electrode surface and dissolve in the alkaline solution owing to its high hydrophilicity. In the presence of graphene, the nickel hydroxide particles become smaller and uniform and interact with graphene tightly based on van der Waals force and endow the electrocatalytic

surface more stable and effective. In an attempt to explore the $Ni(OH)_2$-GN/GC electrode for practical applications, we tested an artificial physiological matrix and spiked samples with different insulin concentrations, i.e. 1 μM, 5 μM, 20 μM on the $Ni(OH)_2$-GN modified biosensor. The recovery and relative standard deviation values are acceptable with a value to be 92.5-105.3%. As a result, the proposed sensor might be promising for the determination of insulin in clinical test.

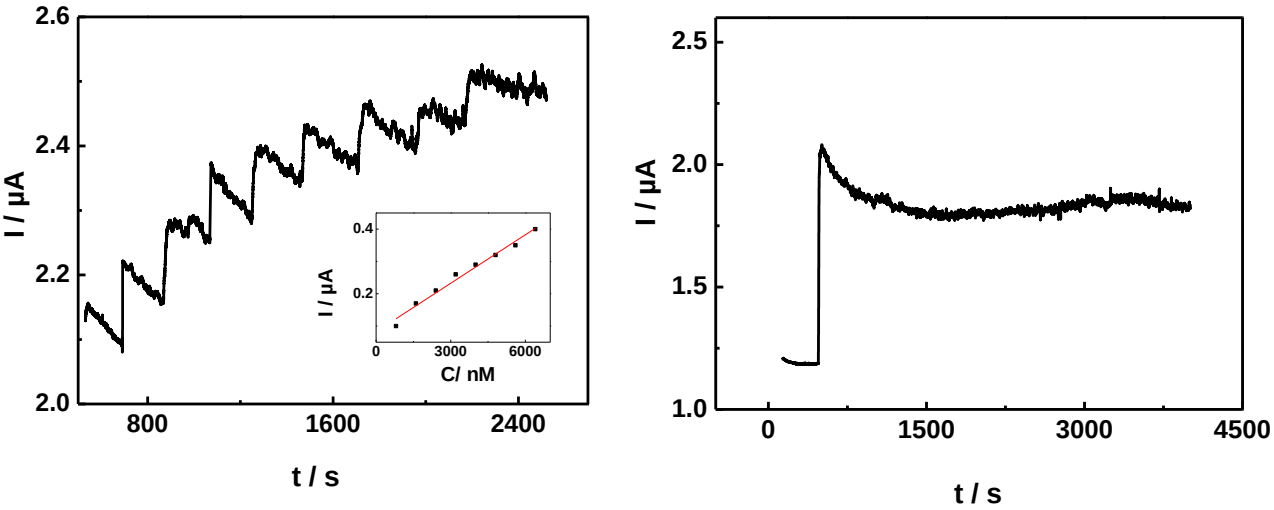

Fig 7. (A) Amperometric response of Graphene-NiOOH /GCE on successive injection of insulin into 0.1 M NaOH solution. Applied potential: 0.51 V. Inset: plot of insulin peak current versus insulin concentration. (B) Stability of the amperometric response to 7 μM insulin during 4000s

Conclusions

In this work, we demonstrate a facile method for in situ growth of $Ni(OH)_2$ nanoparticle on the surface of graphene sheets and a successful example of the detection of insulin based on as-prepared $Ni(OH)_2$-GN modified GC electrode, The prepared electrochemical sensor exhibits much better catalytic performance compared

with pure graphene, with the detection limit of 200 nM and the linear range from 0.8 μM to 6.4 μM. The proposed method was also successfully applied for the determination of insulin in human blood serum sample. High sensitivity, fast response and ease of preparation make this sensor promising for the applications in the development of detecting some other proteins and amino acids.

Acknowledgment This work was financially supported by National Natural Science Foundation (21375088), Scientific Research Project of Beijing Educational Committee (KM201410028006), Scientific Research Base Development Program of the Beijing Municipal Commission of Education and the 2013 Program of Scientific Research Foundation for the Returned Overseas Chinese Scholars of Beijing Municipality.

References:

1. J. Y. Gerasimov, C.S. Schaefer, W. Yang, R.L. Grout and R. Lai, *Biosens. Bioelectron.*, 2013, **42**, 62-68.
2. M. Zhang, C. Mullens and W. Gorski, *Anal. Chem.*, 2005, 77, 6396-6401.
3. Y. Wang and J. Li, *Anal. Chim. Acta*, 2009, **650**, 49-53.
4. B. Rafiee and A. R. Fakhari, *Biosens. Bioelectron.*, 2013, **46**,130–135.
5. B. B. Prasad, R. Madhuri, M. P. Tiwari and P. S. Sharma, *Electrochim. Acta*, 2010, **55**, 9146-9156.
6. S. Wild, G. Roglic, A. Green, R. Sicree and H. King, *Diabetes. Care.*, 2004, **27**, 1047-1053.
7. A. Salimi, A. Noorbakhash, E. Sharifi and A. Semnani, *Biosens. Bioelectron.*, 2008, **24** ,792-798.
8. A. Salimi, L. Mohamadi, R. Hallaj and S. Soltanian, *Electrochem. Commun.*, 2009, **11**, 1116-1119.
9. M. Jaafariasl, E. Shams and M. K. Amini, *Electrochim. Acta*, 2011, **56**, 4390-4395.
10. J. Wang, T. Tangkuaram, S. Loyprasert, T. Vazquez-Alvarez, W. Veerasai, P.Kanatharana, P.Thavarungkul, *Anal. Chim. Acta*, 2007, **581**, 1-6.
11. A. Salimi and R. Hallaj, *J. Solid. State. Electrochem.*, 2012, **16**, 1239-1246.
12. L. Mercolini, A. Musenga, B. Saladini, F. Bigucci, B. Luppi, V. Zecchi and M.A. Raggi, *J. Pharmaceut. Biomed.*, 2008, **48**, 1303-1309.
13. A. Arvinte, A. C. Westermann, A. M. Sesay and V. Virtanen, *Sens. Actuator*

B-Chem., 2010, **150**, 756-763.

14. S. Regonda, R. Tian, J. Gao, S. Greene, J. Ding and W. Hu, *Biosens. Bioelectron.* 2013, **45**, 245-251.
15. M. Quintana, E. Vazquez and M, Prato, *Acc. Chem. Res.*, 2013, **46**, 138-148.
16. F. Long, A. Zhu, H. Shi, H. Wang, *Anal. Chem.*, 2014, **86**, 2862-2866.
17. X. Wang, J. Wang, H. Cheng, P. Yu, J. Ye and L. Mao, *Langmuir*., 2011, **27**, 11180-11186.
18. J. Zhu, M. Chen, Q. He, L. Shao, S. Wei and Z. Guo, *RSC Adv.*, 2013, **3**, 22790-22824.
19. H. Zhou, X. Wang, P. Yu, X. Chen and L. Mao, *Analyst.*, 2012, **137**, 305-308.
20. E. Asadian, S. Shahrokhian, A.I. zad and E. Jokar, *Sens. Actuators*, *B*, 2014, **196**, 582-588.
21. C. Chung, Y-K. Kim, D. Shin, S-R. Ryoo, B. Hong and D-H. Min, *Acc. Chem. Res.*, 2013, **46**, 2211-2224.
22. H. Wang, J.T. Robinson, G. Diankov and H. Dai, *J. Am. Chem. Soc.*, 2010, **132**, 3270-3271.
23. J. Bai and X. Jiang, *Anal. Chem.*, 2013, **85**, 8095-8101.
24. X. Zhu, Y. Zhong, H. Zhai, Z. Yan and D. Li, *Electrochim. Acta*, 2014, **132**, 364-369.
25. X. Niu, Y. Li, J. Tang, Y. Hu, H. Zhao and M. Lan, *Biosens. Bioelectron.*, 2014, **51**, 22-28.
26. P. Si, Y. Huang, T. Wang and J. Ma, *RSC Adv.*, 2013, **3**, 3487-3502.

27. W. Cheng, J. Sue, W. Chen, J. Chang and J. Zen, *Anal. Chem.*, 2010, **82**, 1157-1161.

28. Z. Fan, B. Liu, Z. Li, L. Ma, J. Wang and S. Yang, *RSC Adv.* 2014, **4**, 23319-23326.

29. Y. Miao, L. Ouyang, S. Zhou, L. Xu, Z. Yang, M. Xiao and R. Ouyang, *Biosens. Bioelectron.*, 2014, **53**, 428-439.

30. T.E.M. Nancy and V.A. Kumary, *Electrochim. Acta*, 2014, **133**, 233-240.

31. P. R. Dalmasso, M. L. Pedano and G.A. Rivas, *Sens. Actuators, B*, 2012, **173**, 732-736.

32. A. Ciszewski, K. Sron, L. Stepniak and G. Milczarek, *Electrochim. Acta*, 2014, **134**, 355-362.

33. H. Wang, H. S. Casalongue, Y. Liang and H. Dai, *J. Am. Chem. Soc.*, 2010, **132**, 7472-7477.

34. Y. Xu, X. Huang, Z. Lin, X. Zhong, Y. Huang and X. Duan, *Nano Res.*, 2013, **6**, 65-76.

35. Y. Zhang, F. Xu, Y. Sun, Y. Shi, Z. Wen and Z. Li, *J. Mater. Chem.*, 2011, **21** ,16949-16954.

36. Handbook of Monochromatic XPS Spectra - Vol. 1 - The Elements and Native Oxides, 1999 XPS International, Inc. B. V. Crist, XPS International, Inc., 1999

37. P. Jeevanandam, Y. Koltypin and A. Gedanken, *Nano Lett.*, 2001, **1**, 263-268.

38. Z. Chen, J. Nai, H. Ma and Z. Li, *Electrochim. Acta*, 2014, **116**, 258-262.